

# Conformal Coating of Mammalian Cells Immobilized onto Magnetically Driven Beads

ALI KHADEMHOSEINI,<sup>1-3</sup> MICHAEL H. MAY,<sup>4</sup> and MICHAEL V. SEFTON<sup>2</sup>

## ABSTRACT

A novel cell bead system, comprising a magnetic core, a spherical annulus of agarose-immobilized cells, all conformally coated within a synthetic polymer, is proposed as a means of immunisolating mammalian cells in a system that provides a balance between low total implant volume, retrievability, and diffusion limitations. A successful immunoisolation system could be used to transplant cells without eliciting an inappropriate host response. Chinese hamster ovary (CHO) cells were immobilized at the periphery of large (~2 mm) agarose beads containing inert magnetic cores ( $\leq 1$  mm) and coated in a hydroxyethyl methacrylate–methyl methacrylate (HEMA–MMA) copolymer by interfacial precipitation. The beads were coated in liquid gradients containing polyethylene glycol 200 (PEG) or bromooctane. Although many cells were adversely affected by the coating process, the cells that did survive (30–50% of those loaded into the beads) remained viable for a period of at least 2 weeks. This viability was much higher than achieved previously because of a number of factors, such as the aqueous agarose, the hydrophobic bromooctane intermediate layer, and faster coating times that minimize the exposure of the cells to organic solvents. Also, a mathematical model was used to describe oxygen transport within the annular agarose beads. These results provide evidence that the proposed geometry and the fabrication approach may be useful for a variety of applications that involve cell encapsulation.

## INTRODUCTION

IMMUNOISOLATION OF MAMMALIAN CELLS inside a polymeric membrane is a method of protecting allogeneic and xenogeneic cells from the host's immune system.<sup>1,2</sup> However, clinical applications of immunoisolation have been limited for various reasons, related both to the method of isolation and to the host's response to the implanted tissue. For example, problems include unrealistic implant volumes, low *in vivo* cell viability, as well as diffusion and oxygen limitations.<sup>3</sup>

We have focused on a method of immunisolating the cells within 400- $\mu\text{m}$  (or larger) microcapsules,<sup>4-7</sup> using synthetic, water-insoluble polymers and organic solvents. Somewhat more recently we started exploring a conformal coating process,<sup>4,8</sup> in which the surface of a cell aggregate is coated with a layer of polymer, which conforms to the shape of the aggregate, leading to low total implant volumes. Microcapsules and coated aggregates are small, giving them a high ratio of surface area to (total implant) volume, and so are considered advantageous from a mass transfer perspective. On the other hand,

<sup>1</sup>Division of Biological Engineering, Massachusetts Institute of Technology, Cambridge, Massachusetts.

<sup>2</sup>Department of Chemical Engineering and Applied Chemistry and Institute of Biomaterials and Biomedical Engineering, University of Toronto, Toronto, ON, Canada.

<sup>3</sup>Present address: Division of Biological Engineering, Massachusetts Institute of Technology, Cambridge, Massachusetts.

<sup>4</sup>Rimon Therapeutics, Toronto, ON, Canada.

macrocapsules (capsules that are larger than 1 mm) are advantageous with respect to retrievability and scalability but appear to be limited because of their low surface area-to-volume ratios.<sup>9</sup>

Here, we propose that a conformally coated annulus of cells immobilized within an aqueous polymer matrix that surrounds an inert core may provide a balance among mass transfer constraints, total implant volume, cell viability, and fast response times (Fig. 1). By placing the cells at the periphery of the bead, they can be provided with sufficient oxygen and nutrients, despite the large overall diameter. An additional feature of the particular design proposed here is the magnetic core, which further facilitates retrieval because the iron oxide-rich core can respond to external magnetic forces.

In this article a technique is described with potential applications ranging from immunoisolation to cell-based bioreactors. Cells were immobilized in spherical annular agarose gels that provide an aqueous and three-dimensional environment for the cells. To enable some immune protection, in these studies we conformally coated the agarose–inert core beads with a hydroxyethyl methacrylate–methyl methacrylate copolymer (HEMA–MMA) copolymer, identical to what we have used previously. In the earlier conformal coating process,<sup>4,8</sup> cell aggregates were coated with HEMA–MMA by centrifuging cell aggregates through a liquid density gradient composed of organic and aqueous layers. The particle-induced deformation of the liquid–liquid interface resulted in the cells being entrained in a polymer solution, which precipitated on contact with an aqueous layer. This created a thin protective membrane around the cells, which added little to the overall implant volume. However, because the process was driven by buoyancy forces, it was limited to liquids with low interfacial tensions. Here we extended that process to use magnets, instead of gravity, to drive the beads through liquids with higher interfacial tensions and to drive them faster. In the earlier process, the slow transit through the system and intimate contact between cells and toxic organic liquids resulted in poor cell viability. The use of magnetic forces resulted in faster coating and, as we report here, higher but still limited viability. Selective withdrawal,<sup>10</sup> direct polymerization,<sup>11,12</sup> and centrifugation<sup>8,13</sup> have been used to coat cells through liquid–liquid interfaces. To our knowledge, this is the first demonstration of the use of magnetic forces to encapsulate cells at liquid interfaces.

## MATERIALS AND METHODS

### Magnetic bead preparation

Magnetic polystyrene beads were prepared by modifying the existing microencapsulation process.<sup>14</sup> A mix-

ture of 50:50 (w/w) polystyrene (Sigma, St. Louis, MO) and 0.2- $\mu\text{m}$ -diameter iron oxide powder (Polysciences, Warrington, PA) was dissolved in 10% (w/w) *N,N*-dimethyl formamide (DMF; Sigma-Aldrich, St. Louis, MO). This mixture was extruded through the 22-gauge needle of the microencapsulation assembly at a flow rate of 0.18 mL/min.<sup>6</sup> The resulting drops were sheared by flowing hexadecane through the outer annulus of the encapsulation nozzle into a precipitation bath, where the DMF solvent was extracted, generating beads ( $\sim 750$ – $1100$   $\mu\text{m}$  in diameter). The beads were subsequently washed with sterile phosphate-buffered saline (PBS) and stored overnight at room temperature.

To immobilize Chinese hamster ovary (CHO) cells (American Type Culture Collection [Manassas, VA],

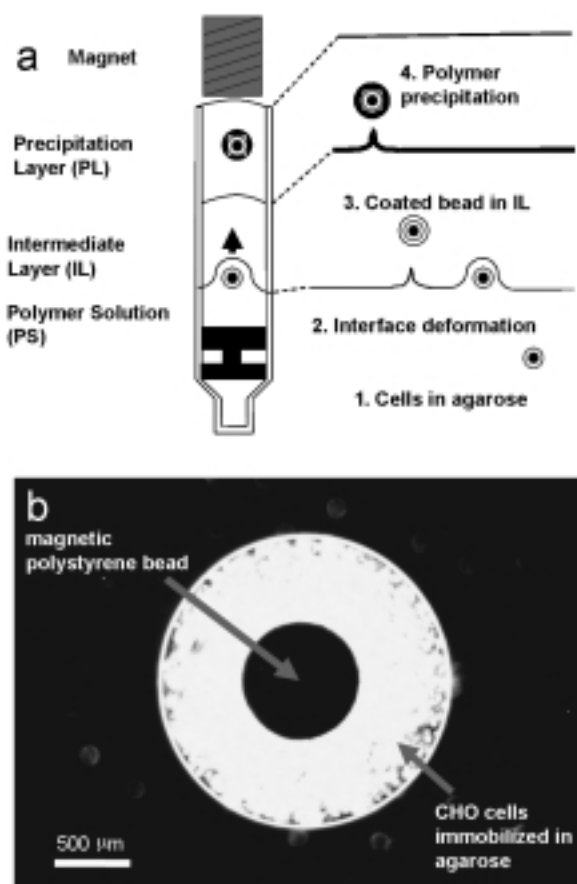


**FIG. 1.** (a) The three-layer liquid gradient was composed of a lower layer of HEMA–MMA dissolved in PEG (PS), an intermediate layer (IL), and an aqueous precipitation layer (PL). The gradients were set up in a syringe barrel and the magnet was kept at a constant distance from the agarose bead by keeping the magnet clamped and moving the syringe assembly as the bead ascended through the liquid gradient. (b) Light micrograph of CHO cells immobilized in agarose around a magnetic core at an initial concentration of  $1 \times 10^6$  cells/mL 1 day after immobilization.

maintained at 37°C, 95% air–5% CO<sub>2</sub>, using  $\alpha$ -MEM tissue culture medium containing penicillin–streptomycin [GIBCO; Invitrogen, Carlsbad, CA] and 10% fetal bovine serum [GIBCO] in agarose around the magnetic cores, magnetic beads were mixed with a preheated solution of 2.5% (w/w) low temperature gelling agarose (type VII; Sigma) in PBS (~35°C) containing the appropriate concentration of CHO cells. The resulting mixture was drawn into Tygon tubing (inner diameter, 1/15 in.; Fisher Scientific, Hampton, NH) that was inserted into a 200- $\mu$ L Eppendorf Combitip (Eppendorf North America, Westbury, NY) placed in a repeat pipetter (Eppendorf North America). Ten-microliter aliquots were sheared off the end of the tube by repeated withdrawals from a mineral oil bath (~1 L) that was cooled to 4°C. The nascent agarose beads were washed with PBS to remove any excess mineral oil.

### Conformal coating

To enclose the agarose beads within the polymer coating, the beads were driven magnetically through a three-layer liquid gradient (Fig. 1) composed of a lower layer of polymer solution (PS), an intermediate layer (IL) of bromooctane (Sigma-Aldrich) or polyethylene glycol (PEG), and an upper layer of nonsolvent aqueous solution. The choice of liquid layers was determined by their densities and interfacial tensions.<sup>8</sup> The purpose of the IL was to prevent contact between the polymer and the nonsolvent, which would result in premature precipitation of the polymer. PBS was used as the nonsolvent precipitation layer for gradients composed of PEG ILs, whereas Pluronic L101 surfactant (1500 ppm in PBS; BASF, Ludwigshafen, Germany) was used for the bromooctane IL. The syringes used for conformal coating were specifically prepared to accommodate the centering of the ascending beads through a curved liquid–liquid meniscus. To prepare these syringes the plunger of a 3-mL tuberculin syringe (BD Biosciences, Franklin Lakes, NJ) was detached from its stem and reinserted to act as a plug. The top section of the syringe was then detached (2.4 cm for PEG IL and 1.2 cm for bromooctane IL) from the plunger and a glass tube with the same diameter was attached to replace the removed section (Fig. 1).

Agarose beads were pulled through the coating gradient by rectangular neodymium–iron–boron magnets (5 × 5 × 1 cm; Efston Science, Toronto, ON, Canada). After the liquid gradient was formed, the beads were driven into the polymer solution of 10–15% (w/v) 75:25 HEMA–MMA in PEG. Subsequently, a constant magnetic force was applied to the beads to drive the process by maintaining a fixed distance between the bead and the magnet (Fig. 1a). The entrained polymer surrounding the bead precipitated on contact with aqueous layer to form a membrane. The beads were then washed with PBS and

transferred to cell medium for further incubation and analysis.

### Analysis of the coating process and bead morphology

The bead diameter and the tail configurations were measured with an inverted epifluorescence light microscope. A video camera set perpendicular to the conformal coating syringe, attached to a stereomicroscope (Zeiss 2000-C; Zeiss, Oberkochen, Germany) and a TV and VCR (Sony, Tokyo, Japan), were used to view and record the movement of the magnetic bead through the liquid gradient.

For scanning electron microscopy (SEM), agarose beads were washed and fixed in 3.5% glutaraldehyde solution (Polysciences). Samples were then immersed in liquid nitrogen and freeze-dried (Lyph-Lock 6; Labconco, Kansas City, MO) for 48 h. On retrieval, some beads were cracked to obtain a cross-sectional view of the coatings. The samples were then viewed with a Hitachi (Tokyo, Japan) S520 scanning electron microscope.

### Cell viability

The metabolic activity of the CHO cells within each coated bead was determined by using a modified version of the previously described 3-(4,5-dimethylthiazol-2-yl)-2,5-diphenyltetrazolium bromide (MTT; Sigma-Aldrich) assay.<sup>15</sup> An agarose bead was placed in each well of a 96-well plate (Corning, Corning, NY) containing 100  $\mu$ L of tissue culture medium and 25  $\mu$ L of MTT (5 mg/mL) dissolved in PBS. The plate was incubated at 37°C for 5 h, after which the beads were washed and dissolved in 200  $\mu$ L of dimethyl sulfoxide (DMSO; Sigma-Aldrich) and stirred on an orbital shaker (Barnstead International, Dubuque, IA) at 100 rpm for 10 min. The color intensity of the solution was determined and quantified with a microplate photometer (MR-700; Dynex Technologies, Berlin, Germany).

To determine cell counts per agarose bead, the beads were cut into smaller pieces. These pieces were dispersed in agarose solution (200 U/mL; Sigma-Aldrich) and incubated for 2 h at 37°C. Subsequently, the cells were trypsinized, washed, and counted after trypan blue exclusion.

Fluorescent viability stains, calcein-AM, and ethidium homodimer-1 (LIVE/DEAD assay; Invitrogen Molecular Probes, Eugene, OR), were used to identify dead and live cells within the agarose beads. Two to four agarose beads were washed in PBS for 15 min and incubated in a 96-well plate at 37°C and 95% air–5% CO<sub>2</sub> for 30 min in 300  $\mu$ L of a 30  $\mu$ M solution of each stain in serum-free  $\alpha$ -MEM. The beads were washed and cut open with a surgical blade under a stereoscopic microscope (Wild Heerbrugg, Heerbrugg, Switzerland). Subsequently,

**TABLE 1. PARAMETER VALUES FOR MODELING OXYGEN CONCENTRATIONS WITHIN BEADS**

Parameter	Value	Ref.
$k$	$3.6 \times 10^{-16}$ mol/cell $\cdot$ s	27
$D$	$2 \times 10^{-9}$ m <sup>2</sup> /s	27
Bulk oxygen concentration	$9 \times 10^{-4}$ mol/L	28, 29

coated cells were examined under an inverted epifluorescence microscope (Axiovert 135; Carl Zeiss, Oberkochen, Germany).

### Simulation of oxygen concentration profile inside the beads

Cell growth in aggregates and beads is limited by nutrient and oxygen diffusion. Therefore, the size of the agarose beads as well as the magnetic core was selected to ensure that the diffusion gradient across the immobilized cell annulus did not result in the formation of necrotic tissue. To obtain the maximum viable cell loading per bead, the process of oxygen transport into the immobilized cell was modeled mathematically. In a simple zero-order model, oxygen transport involves simultaneous diffusion and consumption:

$$\frac{\partial c}{\partial t} = D \frac{1}{r^2} \frac{\partial}{\partial r} \left( r^2 \frac{\partial c}{\partial r} \right) - kb \quad (1)$$

where  $c$  is oxygen concentration in the bead (mol/L),  $D$  is diffusivity of oxygen in the agarose bead (m<sup>2</sup>/s),  $k$  is the oxygen consumption rate (mol/cell  $\cdot$  s), and  $b$  is cell density in the bead (cells/cm<sup>3</sup>). The steady state solution ( $\partial c/\partial t = 0$ ) of Eq. (1) describes the oxygen concentration profile inside the bead for various values of  $b$  and for various agarose and bead dimensions.

Simulations were carried out with Mathematica 3.0 (Wolfram Research, Champaign, IL) with parameter values specified in Table 1. The boundary conditions for the system were as follows: no oxygen flux at the magnetic core–agarose interface, and the oxygen concentration at the bead surface is nearly equal to the bulk oxygen con-

centration (considering that the polymer membrane size is small compared with the bead, and the polymer membrane has a high permeability to oxygen).<sup>16</sup>

## RESULTS

### Cell immobilization and conformal coating

Using the process described above, CHO cells were immobilized around magnetic polystyrene beads (Fig. 1b). Agarose beads that were approximately 2–2.5 mm in diameter within which magnetic beads ( $\sim 750$ – $1000$   $\mu$ m) were well centered were selected for conformal coating. The size of the magnetic cores and agarose beads was adjusted through changes in the shearing force (i.e., hexadecane flow rate) and viscosity<sup>6</sup> of the solutions (data not shown).

In initial studies<sup>4,16</sup> with a buoyancy-driven conformal coating, this process was limited to low liquid–liquid surface tensions; thus, the use of a hydrophobic IL (such as bromooctane) was not possible. The bromooctane–PS interface tension was  $\sim 3.6$  dyn/cm (ring tensiometer; CSC Scientific, Fairfax, VA), compared with  $\sim 10^{-2}$ – $10^{-3}$  dyn/cm for a PEG IL–PS interface. Unlike the buoyancy-driven technique, magnetic forces were sufficient to overcome the interfacial tension. Magnetically driven agarose beads were successfully coated, using both bromooctane and PEG liquid gradients. Figure 2 shows the movement of the agarose/magnetic bead through a PEG IL with a 10% HEMA–MMA PS layer. The beads decelerated as they moved through the liquid–liquid interfaces. The extent of deceleration was dependent on the interfacial tension as well as the applied magnetic force. Not surprisingly, the viscosity of the polymer solution had a direct effect on the velocity of the ascending beads. For example, the beads moved faster through the 10% HEMA–MMA PS layer than through the more viscous 15% HEMA–MMA PS layer.

Both PEG and bromooctane ILs produced uniform coatings ranging from 30 to 70  $\mu$ m depending on the liquid gradient composition and the polymer concentrations (Fig. 3). These coatings were thicker than the coatings



**FIG. 2.** Video images of the magnetically driven conformal coating process in a gradient composed of 10% HEMA–MMA in PEG (polymer solution, PS), a PEG intermediate layer (IL), and a PBS precipitation layer (PL). (a) Bead as it deforms the PS–IL interface and entrains polymer ( $t = 5$  s); (b) bead as it passes through the IL–PL interface ( $t = 7$  s); (c) precipitation of the coating in the PL ( $t = 15$  s)

AU3

T1

F2

F3

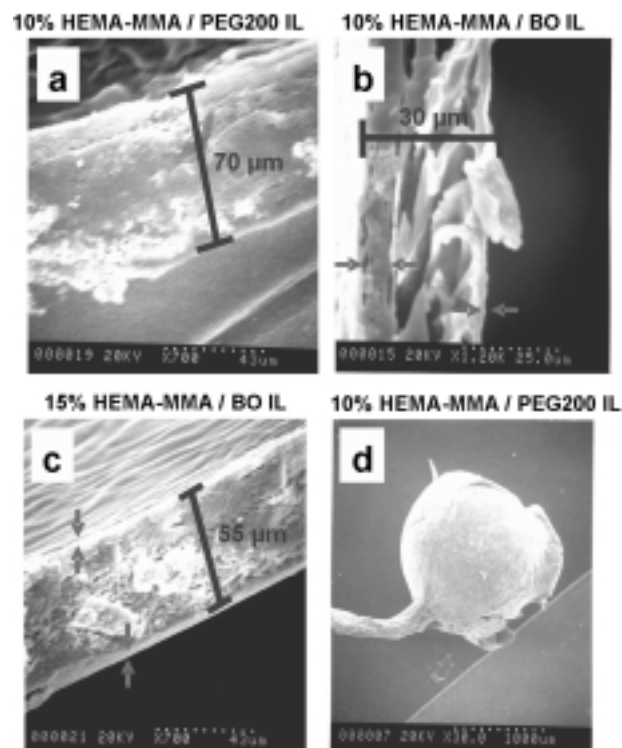


**FIG. 3.** Scanning electron micrographs of HEMA–MMA coatings. The gradient consisted of 10% (w/v) polymer dissolved in PEG with a PEG (a) or bromooctane (BO) (b) intermediate layer and 15% (w/v) polymer dissolved in PEG with a PEG intermediate layer (c). Red arrows show the membrane skin at the surface of membranes formed when using the bromooctane IL. (d) Scanning electron micrograph of a coated bead in 10% HEMA–MMA with a PEG intermediate layer, 1 day after the coating process. Beads were uniformly coated (the cracks on the coatings were due to handling during preparation for SEM).

AU5

previously attained by the buoyancy-driven conformal coating process (5–15 μm).<sup>16</sup> Bromooctane with 10% HEMA–MMA resulted in ~30-μm-thick coatings (Fig. 3c) while the PEG IL using the same polymer concentration produced coatings of ~50 μm (Fig. 3b). As expected, the coating thickness also increased from ~50 to ~75 μm when the polymer concentration was increased from 10 to 15% HEMA–MMA using PEG IL (Fig. 3a and b). Similarly, the morphology of the coatings was dependent on the intermediate layer used for the coating process. In comparison with the PEG IL, bromooctane produced membranes containing a region of macropores, which resembled the HEMA–MMA microcapsule walls (Fig. 3c).<sup>5</sup> Most coatings contained a tail that was formed by precipitation of the draining polymer (Fig. 3d). The tails formed with PEG were typically longer (1.8 ± 0.3 mm) than the tails resulting from the use of bromooctane (0.3 ± 0.2 mm).

*Cell viability*

Despite the presence of organic solvents, a large fraction of the cells remained viable after coating: ~50 and ~30% for bromooctane and PEG intermediate layers, respectively (Fig. 4). The LIVE/DEAD cell assay also detected the presence of a large fraction of viable cells after coating (Fig. 5). The cell viability seen here is a significant improvement over the buoyancy-driven coating process, in which cell viability was undetectable in PEG-based liquid gradients.<sup>8,16</sup> There was no further loss (or gain) in MTT absorbance or cell number during the subsequent 2 weeks of culture. The problem of cell viability is discussed further below.

F4  
F5

*Mathematical modeling*

We performed mathematical modeling of the zero-order reaction and diffusion of oxygen within the agarose region of the microcapsules. The aim of this model was

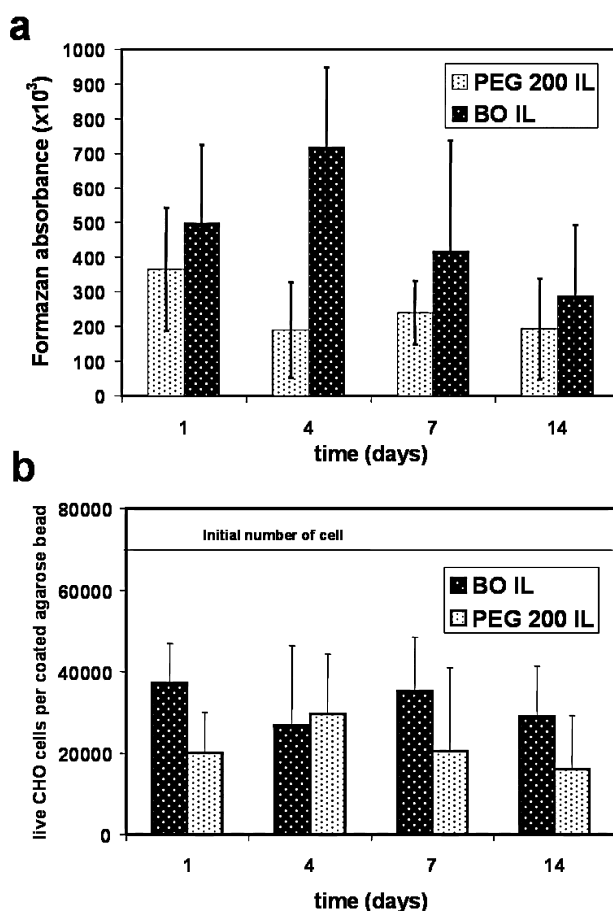


**FIG. 4.** (a) Metabolic activity (MTT) and (b) cell counts of agarose beads containing CHO cells immobilized at an initial concentration of  $5 \times 10^6$  cells/mL and then conformally coated in HEMA–MMA with a bromooctane (BO) or PEG intermediate layer. The cell count was determined by enzymatic digestion of the agarose and subsequent counting with trypan blue.

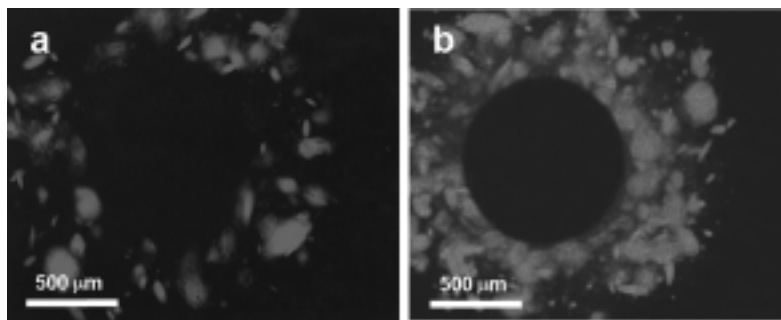


**FIG. 5.** Fluorescence microscopy images of CHO cells immobilized in agarose beads coated through a bromooctane IL, 7 days after the initial coating process. The cells were stained with (a) ethidium homodimer and (b) calcein-AM. Both live (green) and dead (red) cell aggregates are present within the agarose beads.

to predict oxygen concentration at various points in the spherical annulus so that it would not fall below a threshold value that would lead to cell necrosis. To determine the minimum oxygen concentration in which cells remain viable, previous studies regarding neonate rat liver cell aggregates were used.<sup>17</sup> This limit was then set as a threshold value for minimum oxygen concentration that is indicated by the horizontal lines in Figs. 6 and 7. This value provides a conservative criterion for oxygen concentration because liver cells are more metabolically active than other cells such as CHO cells.

As can be seen from the results of simulations exploring the effect of cell density (Fig. 6), for a 2-mm bead and 1-mm core a cell density of  $10^8$ – $10^9$  cells/mL, there is significant oxygen depletion within a small distance ( $<0.2$  mm) from the bead surface. This implies that the cells beyond this distance are in a hypoxic state resulting in the formation of a necrotic annulus. On the other hand, if the cell density is chosen as  $10^6$ – $10^7$  cells/mL, the oxygen concentration remains  $>80\%$  of the surface oxygen concentration throughout the agarose layer, and a necrotic annulus will not likely be formed. If the criterion for an optimum cell density is to use the highest cell concentration in the agarose gel without the cells near the magnetic core becoming hypoxic, then for the analysis here we obtain an optimal cell density of  $2 \times 10^7$  cells/mL.

We also used the simulation to study oxygen concentration in response to modifications to other parameters such as bead size and magnetic core size. Here, we aimed to limit the number of variable parameters by choosing high and low values for the size of the agarose bead (1 or 0.1 mm) and the cell concentration ( $10^7$  or  $10^9$  cells/mL). Then, on the basis of these design criteria, the oxygen concentration within the agarose beads was calculated given different diameters of the magnetic core. The oxygen profiles inside beads of various dimensions are shown in Fig. 7. These results may be used to deter-

mine optimized design parameters based on a specific set of constraints such as the minimum size of a magnetic particle required to generate sufficient magnetic forces to move the particle through the gradient, and the minimum oxygen concentration (i.e.,  $>3.5 \times 10^{-4}$  M) within the beads. Some magnetic core diameters as calculated from these results are shown in Table 2.

T2

## DISCUSSION

There were two aspects to this work: (1) extending a conformal coating encapsulation process to use magnetic force instead of gravity with a view to increasing encapsulated cell viability, and (2) exploring a novel macrobead alternative to microcapsules for the purpose of cell transplantation.

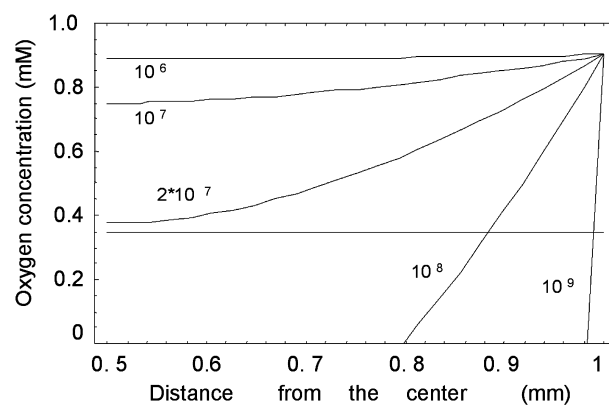


**FIG. 6.** Simulated oxygen concentration profiles for various cell densities (cells/mL) in a 2-mm-diameter bead with a 1-mm-diameter acellular magnetic core. The horizontal line at an oxygen concentration of  $3.5 \times 10^{-4}$  M is the minimum desired oxygen concentration for cells. Higher cell densities result in a low oxygen concentration at the interface between the magnetic core and the agarose layer.

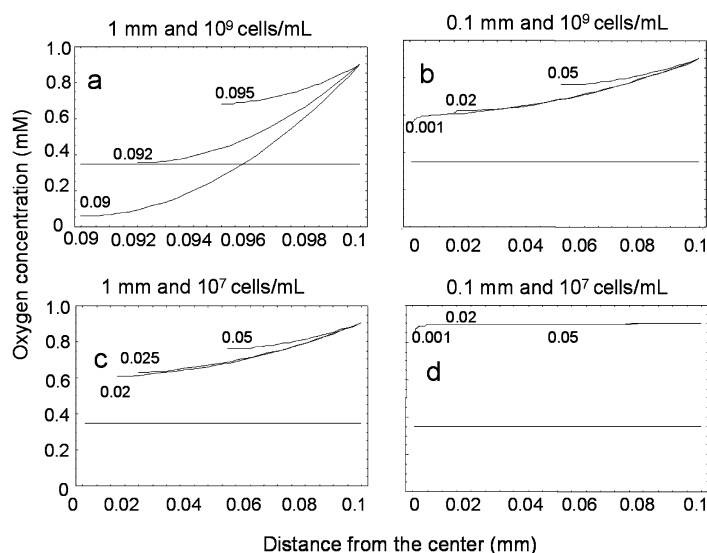


**FIG. 7.** Oxygen concentration profile within the agarose hydrogel for various sizes of agarose beads, magnetic core sizes, and cell densities. Lines are for different magnetic core radii. The horizontal line at an oxygen concentration of  $3.5 \times 10^{-4}$  M is the minimum desired oxygen concentration for cells.

### Conformal coating

In using water-insoluble polymers such as HEMA–MMA for encapsulation, a key consideration has always been to minimize the exposure of cells to organic solvents, which are generally toxic to cells. In the conformal coating process described here, reducing the contact time between the beads and the organic solvents was achieved by moving the beads through the coating layers faster, with the help of a magnetically driven inert core. Agarose also provided an additional diffusion barrier for these organic solvents, thereby reducing their effective concentration. Bromooctane, being hydrophobic, presumably further repelled the hydrophilic agarose beads and created an interfacial barrier. On the other hand, the hydrophilic PEG IL diffused into the agarose beads, consistent with the lower viability of the coated cells with this intermediate layer. The presence of PEG in the polymer solution in both cases likely accounts for the remainder of the viability loss. This is discussed further below.

As expected, interfacial tensions, precipitation rate, and viscosity are the critical parameters in determining the thickness of the coating. As the beads were driven through the interfaces with high interfacial tensions, the increased drainage of the polymer film surrounding the bead significantly reduced the coating thickness. In addition, a more viscous polymer deforms the interface easily, and drags a thicker film through the IL. Because of the increased viscosity of the polymer, less PS is drained at the precipitation interface, resulting in thicker coatings.

The observed differences in membrane structure be-

tween the two ILs (Fig. 3a–c) can be attributed to the consequences of phase inversion. During polymer precipitation, there is an exchange of solvent for nonsolvent. As the nonsolvent concentration in the polymer film surrounding the bead increases, phase separation occurs. In this system the high interfacial tensions with bromooctane caused the entrapped polymer solution to become immediately exposed to the nonsolvent at the bromooctane–PBS interface, which consequently forms a dense layer (the membrane skin). The nascent membrane skin presented resistance to diffusion of the solvent and controlled subsequent sublayer formation. Further precipitant permeation caused nucleation and growth of finger-like cavities (macrovoids) under the skin, as we have seen in conventional microencapsulation.<sup>5</sup> A similar dense

**TABLE 2.** CALCULATED MAGNETIC CORE SIZES FOR VARIOUS COMBINATIONS OF CELL DENSITIES AND AGAROSE BEAD SIZES AS OBTAINED FROM SIMULATIONS SHOWN IN FIG. 7<sup>a</sup>

Agarose bead diameter (mm)	Magnetic core size	
	$10^9$ cells/mL	$10^7$ cells/mL
1	0.92 mm	200 $\mu$ m
0.1	1 $\mu$ m	1 $\mu$ m

<sup>a</sup>The constraints for the system are to keep a minimum 200- $\mu$ m or 1- $\mu$ m magnetic core size for agarose beads of 1 mm or 100  $\mu$ m, respectively (to provide sufficient magnetic forces to drive the beads through the gradients), while keeping the oxygen concentration above  $3.5 \times 10^{-4}$  M.

permeable polymer membrane was formed on the agarose side because of its aqueous nature. In PEG ILs, there are no defined interfaces in the liquid gradient, and therefore the phase inversion process is slower and a different cross-sectional morphology is obtained without the presence of the macrovoids and a membrane skin.

### Geometric considerations

In most therapeutic applications involving immunoisolated cells it is desired to minimize the volume of the implanted tissue while providing the required function. There is also a desire to retrieve these implants once they have served their therapeutic lifetime. This creates a dilemma in the size of immunoisolation devices. On the one hand, many small microcapsules are preferred as they provide a high surface area-to-volume ratio and lower the implant volume, but larger macrocapsules are desired because they are easier to retrieve. The approach presented here aims to balance these two needs. To enhance the retrievability of the capsules, large beads are used to facilitate their recovery because of their size and magnetic properties. To minimize oxygen and nutrient mass transport limitations, the cells are immobilized near the surface of the implant in a spherical annulus: the cells are immobilized in the periphery of the sphere with an inert, impermeable core. Other geometric shapes (such as a cylindrical annulus) may also be suitable, although ease of implantation can be another constraint. In addition to being magnetic, the inert core may have other properties such as controlled release of molecules or imaging modalities that could be used to track the implants. Also of note is that because the cells are immobilized to the periphery of a sphere, a large fraction of the volume of the sphere is occupied by cells, which serves to minimize the total implant volume.

This counterintuitive bead structure is similar to some extent to the agarose macrocapsules proposed by others<sup>18,19</sup> for islet immunoisolation. Although those agarose beads did not have an inert core, they did exploit the same geometric advantage. Each larger “capsule” occupies more volume than a smaller capsule so that few macrocapsules are needed for the same dose of cells, assuming there is no internal diffusion limitation.

The mathematical model, on which this spherical annulus design is based, is admittedly simple. For example, it does not take into account process limitations, including low cell viability and nonuniform cell distribution within the beads, nor does it model the nonlinear relationship between oxygen concentration and cell function.<sup>20</sup> Also, the parameters used such as oxygen consumption rate, minimum desired oxygen concentration, cell growth rates, and other factors will change depending on the type of cell type used. Additional refinements for the model may be beneficial to improve the predictive behavior of the model.

### Future scope for improvement

Several difficulties are associated with the magnetically driven coating process, the most important of which is the significant loss of cell viability. Although 30–50% viability retention is not unreasonable for this stage of process development, these values need to be improved substantially if this process is to be practical. One approach to enhancing viability is to reduce the contact time within the layers of the coating process, using stronger magnets. Electromagnets, an increase in the core iron oxide content, or various geometric modifications to focus the magnetic field could potentially solve this difficulty. Interestingly, we have used PEG without a problem in our conventional encapsulation process,<sup>4,21</sup> presumably because the contact time is short (on the order of seconds). In conformal coating the transit time is on the order of minutes, leading to greater toxicity issues.

The extent of cell death may also be reduced with the use of different polymer solvents. Iopamidol, which has been shown to dissolve certain HEMA–MMA copolymers,<sup>22</sup> has been shown to improve cell viability for buoyancy-driven conformal coating experiments.<sup>23</sup> Cell viability, although better than before, is still low and this remains a limitation of this process; ultimately, we envisage the magnetic bead approach to be more useful with other coating polymers. Other difficulties include the slow precipitation of polymer, which leads to excessive drainage of the polymer and nonuniform polymer coating. Glycerol may be added to increase the precipitation rate and prevent rapid drainage of the polymer, and polyvinyl pyrrolidone may be used as a pore-forming agent to modulate permeability.

In this work we used agarose as the matrix for cell immobilization. Agarose has been shown to provide little mass transfer limitation to hydrophilic solutes of molecular masses up to 150 kDa. Also, oxygen diffusivity in agarose was found to be about 95% of those of pure water.<sup>24</sup> Thus, the cells may be expected to remain viable for long periods of time, as they are able to receive nutrition as well as oxygen. The immobilization matrix used in this design provides additional mechanical support and perhaps some additional protection from the immune system (in addition to the HEMA–MMA membrane). Also, as an alternative to agarose, bioactive extracellular matrices or polymers (e.g., Matrigel) may be used to facilitate the immobilization of various cell types. These materials have been used in other microencapsulation processes and provide cells with specific signals that are more representative of the *in vivo* microenvironment.<sup>25,26</sup> In addition, the geometry proposed here can be adapted to other encapsulation polymers such as alginate–polylysine, although each material might need a different conformal coating process.

The system proposed here is useful for both cell transplantation as well as cell-based bioreactors. Clearly, the

proposed approach has potential applications for immunoisolation of mammalian cells for transplantation. Here, we limited the scope of the article to testing the *in vitro* feasibility of the approach and future studies will explore the *in vivo* behavior of the proposed approach. In addition, this approach could be an important tool for culturing cells within stirred bioreactors with the ability to easily retrieve the beads on the basis of their size and magnetic properties. These bioreactor systems will be particularly useful for anchorage-dependent cells because, by incorporating other extracellular matrices (instead of agarose), they provide the cells with cues that may enhance their function.

Finally to facilitate these applications the system must be easily scalable. In this article we describe a batch fabrication process that relies on the movement of magnets. However, the technique could be changed to a continuous process by changing the single syringe to a fluidic system in which electrically operated magnetic coils are integrated into the channels to drive multiple beads through the liquid gradients. In addition, the use of a bromooctane IL allows the liquid gradients to be stable over time, in contrast to the PEG density gradients used previously, which also enhances the scalability and reproducibility of the system.

## CONCLUSIONS

CHO cells immobilized to the periphery of large agarose beads containing inert magnetic cores were conformally coated in HEMA–MMA by interfacial precipitation. Magnetic forces were used to drive the beads through a three-layer density gradient composed of a lower layer of polymer solution, an upper layer of nonsolvent, and a separate intermediate layer separating the two phases. The use of magnets has increased the maximum allowable interfacial tension within the gradient from  $10^{-2}$  to  $>3.5$  dyn/cm, enabling the use of bromooctane as the intermediate layer. Also, by replacing the IL with hydrocarbons (such as bromooctane) that were immiscible with both the aqueous and HEMA–MMA layers, cell viability was enhanced, although it was still not as high as needed for full utility. Mathematical modeling was helpful in choosing bead and core diameters as well as in demonstrating the effect of cell density. A novel annular bead structure for cell transplantation devices emerged from the modeling exercise; this structure may ultimately prove useful as a means of enabling high cell doses, low device volumes, and retrievability.

## ACKNOWLEDGMENTS

The authors thank Siddhartha Jain for helpful discussions on mathematical modeling, and the Natural Sci-

ences and Engineering Research Council of Canada and the Canadian Institutes of Health Research for financial support.

## REFERENCES

1. Chang, T.M.S. Semipermeable microcapsules. *Science* **146**, 524, 1964.
2. Lim, F., and Sun, A.M. Microencapsulated islets as a bioartificial endocrine pancreas. *Science* **210**, 908, 1980.
3. Chicheportiche, D., and Reach, G. *In vitro* kinetics of insulin release by microencapsulated rat islets: Effect of the size of the microcapsules. *Diabetologia* **31**, 54, 1988.
4. Sefton, M.V., May, M.H., Lahooti, S., and Babensee, J.E. Making microencapsulation work: Conformal coating, immobilization gels and *in vivo* performance. *J. Control. Release* **65**, 173, 2000.
5. Crooks, C.A., Douglas, J.A., Broughton, R.L., and Sefton, M.V. Microencapsulation of mammalian cells in a HEMA–MMA copolymer: Effects on capsule morphology and permeability. *J. Biomed. Mater. Res.* **24**, 9, 1990.
6. Hwang, J.R., and Sefton, M.V. Effect of capsule diameter on the permeability to horseradish peroxidase of individual HEMA–MMA microcapsules. *J. Control. Release* **49**, 217, 1997.
7. Uludag, H., De Vos, P., and Tresco, P.A. Technology of mammalian cell encapsulation. *Adv. Drug Deliv. Rev.* **42**, 29, 2000.
8. May, M.H., and Sefton, M.V. Conformal coating of small particles and cell aggregates at a liquid–liquid interface. *Ann. N.Y. Acad. Sci.* **875**, 126, 1999.
9. Yang, H., Iwata, H., Shimizu, H., Takagi, T., Tsuji, T., and Ito, F. Comparative studies of *in vitro* and *in vivo* function of three different-shaped bioartificial pancreases made of agarose hydrogel. *Biomaterials* **15**, 113, 1994.
10. Cohen, I., Li, H., Hougland, J.L., Mrksich, M., and Nagel, S.R. Using selective withdrawal to coat microparticles. *Science* **292**, 265, 2001.
11. Sawhney, A.S., Pathak, C.P., van Rensburg, J.J., Dunn, R.C., and Hubbell, J.A. Optimization of photopolymerized bioerodible hydrogel properties for adhesion prevention. *J. Biomed. Mater. Res.* **28**, 831, 1994.
12. Cruise, G.M., Hegre, O.D., Lamberti, F.V., Hager, S.R., Hill, R., Scharp, D.S., and Hubbell, J.A. *In vitro* and *in vivo* performance of porcine islets encapsulated in interfacially photopolymerized poly(ethylene glycol) diacrylate membranes. *Cell Transplant.* **8**, 293, 1999.
13. Zekorn, T., Siebers, U., Horcher, A., Schnettler, R., Zimmermann, U., Bretzel, R.G., and Federlin, K. Alginate coating of islets of Langerhans: *In vitro* studies on a new method for microencapsulation for immuno-isolated transplantation. *Acta Diabetol.* **29**, 41, 1992.
14. Sefton, M.V., Hwang, J.R., and Babensee, J.E. Selected aspects of the microencapsulation of mammalian cells in HEMA–MMA. *Ann. N.Y. Acad. Sci.* **831**, 260, 1997.
15. Uludag, H., and Sefton, M.V. Colorimetric assay for cellular activity in microcapsules. *Biomaterials* **11**, 708, 1990.
16. May, M.H. Ph.D. thesis. University of Toronto, Toronto, ON, Canada, 1998.

17. Landry, J., Bernier, D., Ouellet, C., Goyette, R., and Marceau, N. Spheroidal aggregate culture of rat liver cells: Histotypic reorganization, biomatrix deposition, and maintenance of functional activities. *J. Cell Biol.* **101**, 914, 1985.
18. Jain, K., Yang, H., Asina, S.K., Patel, S.G., Desai, J., Diehl, C., Stenzel, K., Smith, B.H., and Rubin, A.L. Long-term preservation of islets of Langerhans in hydrophilic macrobeads. *Transplantation* **61**, 532, 1996.
19. Jain, K., Yang, H., Cai, B.R., Haque, B., Hurvitz, A.I., Diehl, C., Miyata, T., Smith, B.H., Stenzel, K., Suthanthiran, M., *et al.* Retrievable, replaceable, macroencapsulated pancreatic islet xenografts: Long-term engraftment without immunosuppression. *Transplantation* **59**, 319, 1995.
20. Dionne, K.E., Colton, C.K., and Yarmush, M.L. Effect of hypoxia on insulin secretion by isolated rat and canine islets of Langerhans. *Diabetes* **42**, 12, 1993.
21. Uludag, H., and Sefton, M.V. Microencapsulated human hepatoma (HepG2) cells: *In vitro* growth and protein release. *J. Biomed. Mater. Res.* **27**, 1213, 1993.
22. Morikawa, N., Iwata, H., Matsuda, S., Miyazaki, J., and Ikada, Y. Encapsulation of mammalian cells into synthetic polymer membranes using least toxic solvents. *J. Biomater. Sci. Polym. Ed.* **8**, 575, 1997.
23. Nikhilanandhan, G. M.Sc. thesis. University of Toronto, Toronto, ON, Canada, 1999.
24. Li, R.H., Altreuter, D.H., and Gentile, F.T. Transport characterization of hydrogel matrices for cell encapsulation. *Biotechnol. Bioeng.* **50**, 365, 1996.
25. Lahooti, S., and Sefton, M.V. Effect of an immobilization matrix and capsule membrane permeability on the viability of encapsulated HEK cells. *Biomaterials* **21**, 987, 2000.
26. Lahooti, S., and Sefton, M.V. Microencapsulation of normal and transfected L929 fibroblasts in a HEMA-MMA copolymer. *Tissue Eng.* **6**, 139, 2000.
27. Yarmush, M.L., Dunn, J.C., and Tompkins, R.G. Assessment of artificial liver support technology. *Cell Transplant.* **1**, 323, 1992.
28. Rotem, A., Toner, M., Tompkins, R.G., and Yarmush, M.L. Oxygen-uptake rates in cultured rat hepatocytes. *Biotechnol. Bioeng.* **40**, 1286, 1992.
29. Rotem, A., Toner, M., Bhatia, S., Foy, B.D., Tompkins, R.G., and Yarmush, M.L. Oxygen is a factor determining *in vitro* tissue assembly: Effects on attachment and spreading of hepatocytes. *Biotechnol. Bioeng.* **43**, 654, 1994.

Address reprint requests to:

*Michael V. Sefton, Ph.D.*

*Department of Chemical Engineering and  
Applied Chemistry*

*Institute of Biomaterials and Biomedical Engineering  
University of Toronto*

*4 Taddle Creek Road, Room 407D  
Toronto, Canada M5S 3G9*

*E-mail: sefton@ecf.utoronto.ca*

**KHADEMHOSEINI**

**AU1**

**Please insert degrees for all authors, and postal codes for all affiliations; and check corresponding author degree and address, inserted following references.**

**AU2**

**Preceding OK as set? Or please amend.**

**AU3**

**Preceding OK as “immobilized cell”? Or please amend to clarify meaning.**

**AU4**

**Should give thesis title and department? See also Ref. 23.**

**AU5**

**Please check comments on Fig. 3 in text versus Fig. 3 caption and data presented in Fig. 3 itself; they do not seem to agree in some cases? Apologies if not understanding.**